

Finite-blocklength Fluid Antenna Systems With Spatial Block-Correlation Channel Model

Zhentian Zhang, *Graduate Student Member, IEEE*, Kai-Kit Wong, *Fellow, IEEE*, David Morales-Jimenez, *Senior Member, IEEE*, Hao Jiang, *Member, IEEE*, Pablo Ramírez-Espinosa, *Member, IEEE*, Chan-Byoung Chae, *Fellow, IEEE*, and Christos Masouros, *Fellow, IEEE*

Abstract—Massive connectivity with ultra-low latency and high reliability necessitates fundamental advances in future communication networks operating under finite-blocklength (FBL) transmission. Fluid antenna systems (FAS) have emerged as a promising enabler, offering superior spectrum and energy efficiency in short-packet/FBL scenarios. In this work, by leveraging the simplicity and accuracy of block-correlation channel modeling, we rigorously bound the performance limits of FBL-FAS from a statistical perspective, focusing on two key performance metrics: block error rate (BLER) and outage probability (OP). Furthermore, we introduce a novel complex-integral simplification method based on Gauss-Laguerre quadrature, which achieves higher approximation accuracy compared to existing Taylor-expansion-based approaches. Numerical results validate the robustness of the proposed analysis and clearly demonstrate the superiority of FBL-FAS over conventional multiple-antenna systems with fixed antenna placement.

Index Terms—Fluid antenna systems, finite-blocklength, block-correlation model, block error rate, outage probability, integral simplification, Gauss-Laguerre quadrature.

I. INTRODUCTION

FLUID antenna systems (FAS) represent a communication architecture that achieves substantial spatial diversity gains by dynamically altering radiation characteristics through flexible antenna structures and adaptive protocol designs [1]. Unlike conventional approaches that seek to avoid antenna correlation in compact spaces, FAS intentionally embraces and exploits it to yield significant channel gains [2], thereby enabling robust service quality with reduced hardware overhead and simplified protocol design. Recent work [3] investigated the performance limits of FAS under the finite blocklength (FBL) regime, demonstrating that fluid antennas

can simultaneously secure high spectrum and power efficiency. Furthermore, FBL theories [4], [5] provide both fundamental insights and practical guidelines for system design to meet the requirements of massive access, ultra-low latency, and high reliability. Unlike prior studies that primarily adopt outage probability (OP) as the performance metric for FAS, [3] introduces block error rate (BLER) as a universal and analytically tractable metric with a closed-form expression. The main scope and contributions of this work are summarized as follows:

- In this work, we focus on the FBL-FAS problem [3] under the block-correlation channel model [6] of FAS. With accurate channel modeling, the performance limits of FBL-FAS are statistically characterized by providing tighter upper bounds without requiring prior channel state information (CSI).
- We derive the PDF expression of the channel response after antenna/port selection, which is concisely represented by a non-central chi-square distribution.
- Furthermore, we introduce a more general integral simplification method inspired by the Gauss-Laguerre approach. Compared with the previously used Taylor-expansion-assisted method [3], our method avoids amplified approximation errors from high-order expansion terms under large antenna correlation, and achieves improved approximation accuracy.

The remainder of the paper is organized as follows: In Section II, FBL-FASs under block-correlation channel modeling are explained. Subsequently, our main results are introduced in Section III while explicit derivations are deferred to Section VI. Numerical results are illustrated and explained in Section IV and the conclusion is drawn in Section V.

II. SYSTEM DESCRIPTIONS

In this work, we consider an uplink transmission scenario where a base station (BS) equipped with a conventional single antenna serves U single-antenna user equipments with blocklength M . Each UE employs a fluid antenna with N preset configurable locations/ports that are evenly distributed along a linear array of length W , where W denotes the antenna length normalized by the wavelength at the operating frequency. Each port is regarded as an ideal antenna; however, due to limited hardware resources such as the radio frequency (RF) chain, only one port will be activated at a time.

Z. Zhang and H. Jiang are with the National Mobile Communications Research Laboratory, Southeast University, Nanjing, 210096, China and H. Jiang is also with the School of Artificial Intelligence, Nanjing University of Information Science and Technology, Nanjing 210044, China. (e-mail: zhentianzhangzst@gmail.com, jianghao@nuist.edu.cn).

K.-K. Wong and C. Masouros are with the Department of Electronic and Electrical Engineering, University College London, Torrington Place, WC1E 7JE, United Kingdom (e-mails: {kai-kit.wong, c.masouros}@ucl.ac.uk). K.-K. Wong is also affiliated with the Yonsei Frontier Lab., Yonsei University, Seoul, 03722 South Korea.

D. Morales-Jimenez is with the Department of Signal Theory, Networking and Communications, University of Granada, Granada 18071, Spain (e-mail: dmorales@ugr.es).

P. Ramírez-Espinosa is with Telecommunications Research Institute (TELMA), University of Malaga, 29071 Malaga, Spain (e-mail: pre@ic.uma.es).

C.-B. Chae is with the School of Integrated Technology, Yonsei University, Seoul, 03722 South Korea (e-mail: cbchae@yonsei.ac.kr).

Corresponding authors: K.-K. Wong (kai-kit.wong@ucl.ac.uk)

A. Spatial Block-Correlation Channel Model for Single Antenna N -Ports FAS

Our starting point builds upon the FBL-FAS analytical model in [3], [2]. In contrast, we extend the analysis to incorporate the spatial block-correlation channel model in [6]. Since this channel model differs from that in [3], it is necessary to illustrate how the block-correlation model can be adopted to generate random channel realizations within the FBL-FAS framework. Let $\mathbf{g}_u \in \mathbb{C}^N$ denote the channel coefficient vector of the u -th user, and let $\mathbf{\Sigma} \in \mathbb{C}^{N \times N}$ represent the corresponding spatial correlation matrix. Owing to the even placement of ports, the correlation matrix $\mathbf{\Sigma}$ takes the form of a Toeplitz matrix:

$$\mathbf{\Sigma} = \begin{pmatrix} a(0) & a(1) & a(2) & \dots & a(N-1) \\ a(-1) & a(0) & a(1) & \dots & a(N-2) \\ \vdots & \ddots & \vdots & \ddots & \vdots \\ a(-N+1) & a(-N+2) & \dots & a(-1) & a(0) \end{pmatrix}, \quad (1)$$

where the generation function is:

$$a(n) = \text{sinc}\left(\frac{2\pi nW}{N-1}\right). \quad (2)$$

With correlation matrix $\mathbf{\Sigma}$, one could generate \mathbf{g}_u feasibly via eigenvalue-based construction [1, Eq. 5]:

$$\mathbf{g}_u = \mathbf{Q}\mathbf{\Lambda}^{\frac{1}{2}}\mathbf{g}_0, \quad (3)$$

Here, \mathbf{Q} denotes the matrix of left eigenvectors obtained from the eigenvalue decomposition of the correlation matrix $\mathbf{\Sigma} = \mathbf{Q}\mathbf{\Lambda}\mathbf{Q}^H$, and $\mathbf{g}_0 \in \mathbb{C}^N \sim \mathcal{CN}(\mathbf{0}, \sigma^2\mathbf{I})$. However, directly analyzing the statistical distribution based on $\mathbf{\Sigma}$ is infeasible and overly complicated for any tractable analyses.

Fortunately, the principal components of $\mathbf{\Sigma}$ can be captured by only a small number of dominant eigenvalues and their corresponding eigenvectors [6, Fig. 3], [1]. Hence, the correlation matrix $\mathbf{\Sigma}$ can be approximated by a block-diagonal matrix:

$$\hat{\mathbf{\Sigma}} \in \mathbb{R}^{N \times N} = \begin{pmatrix} \mathbf{A}_1 & \mathbf{0} & \dots & \mathbf{0} \\ \mathbf{0} & \mathbf{A}_2 & \dots & \mathbf{0} \\ \vdots & & \ddots & \vdots \\ \mathbf{0} & \mathbf{0} & \mathbf{0} & \mathbf{A}_B \end{pmatrix}, \quad (4)$$

Each diagonal block \mathbf{A}_b , $b \in \{1, 2, \dots, B\}$, is a constant correlation matrix of size $L_b \times L_b$, satisfying $\sum_{b=1}^B L_b = N$ (omit rounding errors). Intuitively, the correlation matrix characterizes the correlation among neighboring ports, where the correlation is typically strong due to the compact port spacing. The matrix $\hat{\mathbf{\Sigma}}$ represents the fitted approximation of $\mathbf{\Sigma}$ according to [6, Eq. 20], while offering a more convenient structure for analytical treatment. In particular, the block-correlation matrix exhibits the following common form:

$$\mathbf{A}_b = \begin{pmatrix} 1 & \mu_b^2 & \dots & \mu_b^2 \\ \mu_b^2 & 1 & \dots & \mu_b^2 \\ \vdots & & \ddots & \vdots \\ \mu_b^2 & \dots & \mu_b^2 & 1 \end{pmatrix}, \quad (5)$$

where μ_b^2 is the correlation constant. Two important assumptions adopted throughout the remainder of the paper are summarized as follows:

- Without loss of generality, μ_b^2 , $b \in \{1, 2, \dots\}$ are assumed identical, i.e., $\mu_1^2 = \mu_2^2 = \dots = \mu^2 \in (0.95, 0.99)$, as established in [6, Sec. III-B-2).
- The block size L_b is adaptive to the desired approximation accuracy, which follows the procedure in [6, Algorithm 1]. For implementation details, the reader is kindly referred to the open-source code provided therein.

B. Finite-Blocklength Single Antenna FAS Signal Model

Assuming synchronous transmission, U single-antenna users transmit M -length signals, and the received signal can be expressed as

$$\mathbf{y} = g_{i,k}\mathbf{x}_i + \sum_{u \neq i}^U g_{u,k}\mathbf{x}_u + \boldsymbol{\eta}, \quad (6)$$

where \mathbf{x}_u denotes the Gaussian codeword of user u with zero mean and variance $\sigma_c^2 = \frac{1}{M}$, such that $\|\mathbf{x}_u\|_2^2 = 1$. The term $\boldsymbol{\eta}$ represents the additive white Gaussian noise (AWGN) with zero mean and variance $\frac{\sigma^2}{M}$, i.e., $\|\boldsymbol{\eta}\|_2^2 = \sigma_\eta^2$. With a slight abuse of notation, $g_{u,k}$ denotes the k -th channel coefficient of user u , where $k \in \{1, 2, \dots, N\}$. The channel coefficients are Rayleigh distributed with variance σ^2 and correlated by (4). Moreover, the signal-to-noise ratio (SNR) is defined as

$$\text{SNR} = \frac{\mathbb{E}\{\|g_{i,k}\mathbf{x}_i\|_2^2\}}{\mathbb{E}\{\|\boldsymbol{\eta}\|_2^2\}} = \frac{\sigma^2}{\sigma_\eta^2}. \quad (7)$$

III. MAIN RESULTS

In this section, we derive the PDF of the random variable $|g_{\text{FAS}}|^2 = \max\{|g_{u,1}|^2, |g_{u,2}|^2, \dots, |g_{u,N}|^2\}$, based on which both the *conditional* BLER (with known channel response) and the *statistical* BLER (without prior CSI) are obtained. Furthermore, we investigate the outage OP expressions of FBL-FAS under the block-correlation channel model. In addition, we clarify why the integral simplification method in [3, Eq. 52], i.e., the Taylor-expansion-assisted mean value theorem for integrals, is not applicable to the block-correlation model. Instead, we propose a tailored simplification approach for block correlation model based on Gauss–Laguerre quadrature.

A. PDF of $|g_{\text{FAS}}|^2$ and BLER under Block-Correlation Model

Result 1: The PDF of the random variable $|g_{\text{FAS}}|^2 = \max\{|g_{u,1}|^2, |g_{u,2}|^2, \dots, |g_{u,N}|^2\}$ for FBL-FAS under the block-correlation channel model is given in (8), where $f_{\chi_2^2}(x; \lambda)$ and $F_{\chi_2^2}(x; \lambda)$ denote the PDF and CDF of a non-central chi-square distribution with 2 degrees of freedom and non-centrality parameter λ , respectively.

Proof: See Appendix VI-A. ■

For illustration, the exact CDF in (13), the derived PDF in (8), and the Monte Carlo samples obtained via (3) are plotted in Fig. 1, where the channel model setups are generated with $N = 10$, $\mu^2 = 0.97$, and $W = 0.5$. Notably, consistent with [6], the CDF in (13) assumes $\sigma^2 = 2$, which will be adopted throughout the simulations in this work¹.

¹It is straightforward to extend the CDF and PDF to different variances σ^2 , which can be done by a standard change of variables in the PDF/CDF.

$$f_{|g_{\text{FAS}}|^2}(t) = \sum_{b=1}^B \left\{ \int_0^\infty \frac{e^{-\frac{r_b}{2}} L_b}{2} \left[F_{\chi^2_2} \left(\frac{t}{1-\mu^2}; \frac{\mu^2 r_b}{1-\mu^2} \right) \right]^{L_b-1} \frac{f_{\chi^2_2} \left(\frac{t}{1-\mu^2}; \frac{\mu^2 r_b}{1-\mu^2} \right)}{1-\mu^2} dr_b \right\} \times \prod_{j \neq b}^B \left\{ \int_0^\infty \frac{e^{-\frac{r_j}{2}}}{2} \left[F_{\chi^2_2} \left(\frac{t}{1-\mu^2}; \frac{\mu^2 r_j}{1-\mu^2} \right) \right]^{L_j} dr_j \right\}, \quad (8)$$

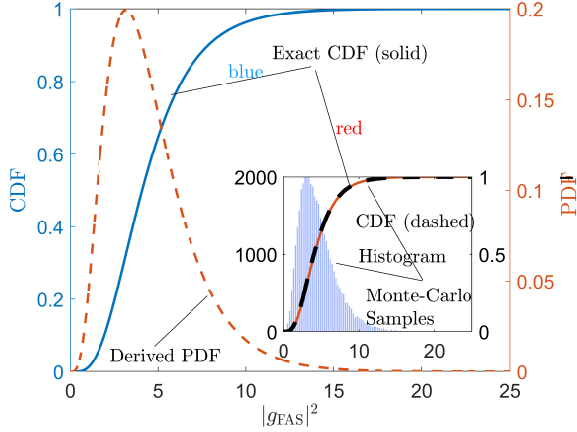


Fig. 1. Illustration of block-correlation model's CDF and the PDF (exact CDF in (13), derived PDF in (8) and Monte-Carlo samples.) with $N = 10$, $\mu^2 = 0.97$, $W = 0.5$.

Remark 1 According to [3, Theorem 5], for FBL-FAS with U codewords to be detected under transmission of M block-length, the BLER can be upperbounded by the *conditional* (known channel response) error probability denoted by ϵ :

$$\epsilon \leq \sum_{U'=0}^U \frac{U'}{U} e^{L'-M \log \left(1 + \frac{0.25\sigma_\eta^2}{\sigma_\eta^2} \right)}, \quad (9)$$

where $L' = \log \left(\frac{U'}{U'} \right)^2 = \sum_{i=1}^{U'-1} \log \frac{U-i}{U'-i}$ and $\sigma_\eta^2 = 2U'\sigma_c^2 |g_{\text{FAS}}|^2$. With the conditional BLER in (9), one could easily obtain the *statistical* BLER (without CSI) denoted by $\bar{\epsilon}$ below:

$$\bar{\epsilon} = \sum_{U'=0}^U \frac{U'}{U} \int_0^\infty f_{|g_{\text{FAS}}|^2}(t) e^{L'-M \log \left(1 + \frac{0.25\sigma_\eta^2}{\sigma_\eta^2} \right)} dt, \quad (10)$$

where $f_{|g_{\text{FAS}}|^2}(t)$ is the PDF of $|g_{\text{FAS}}|^2$ and $\sigma_\eta^2(t) = 2U'\sigma_c^2 t$.

B. SINR-based Outage Probability and Integral Simplification

Remark 2 Let Γ denote the SINR under FBL-FAS and γ_{th} as the OP threshold, in accordance with [3, Appendix H], and let the OP event be defined as:

$$\left\{ \Gamma \leq \gamma_{\text{th}} \right\} = \left\{ |g_{\text{FAS}}|^2 \leq \frac{\sigma_\eta^2 \gamma_{\text{th}}}{1 - (U-1)(U\bar{\rho}+1)\gamma_{\text{th}}} \right\}, \quad (11)$$

where $\bar{\rho} = \sqrt{\frac{\pi}{4M}}$ is the average codeword correlation (please refer to [3, Theorem 3] for details). Hereby, with CDF in (13),

the OP for FBL-FAS under block-correlation channel model is calculated as:

$$p_{\text{out}}^{\text{FBL-FAS}} = \prod_{b=1}^B \int_0^\infty \frac{e^{-\frac{r_b}{2}}}{2} \times \left[1 - Q_1 \left(\sqrt{\frac{\mu^2 r_b}{1-\mu^2}}, \sqrt{\frac{t_{\text{th}}}{1-\mu^2}} \right) \right]^{L_b} dr_b, \quad (12)$$

where $t_{\text{th}} = \frac{\sigma_\eta^2 \gamma_{\text{th}}}{1 - (U-1)(U\bar{\rho}+1)\gamma_{\text{th}}}$. Still, the expression in (12) has an infeasible product-integral structure. We next find an effective method to simplify the calculation.

Result 2: For the integral in (12), the simplification method originally adopted in [3, Theorem 7]—namely, the Taylor-expansion-assisted mean value theorem for integrals—is not applicable to the block-correlation model. *In this work, we propose a novel approach for integral simplification based on Gauss–Laguerre quadrature, tailored to the analysis of FBL-FAS under the block-correlation model.*

Details: See Appendix VI-B. ■

IV. NUMERICAL RESULTS

In this part, we illustrate the BLER and OP performance of FBL-FAS under the block-correlation model. The OP and BLER for a conventional L -antenna scheme using maximum ratio combining (MRC) [3, Section III-D] are included as benchmarks. For the Monte Carlo simulations, random channel realizations are generated according to (3). Unless otherwise specified, the default setup assumes channel variance $\sigma^2 = 2$ (consistent with [6]) and correlation parameter $\mu^2 = 0.97$.

A. BLER and OP Performance

The BLER and OP performance results are illustrated in Fig. 2 and Fig. 3, respectively, with parameter setups and explanations on curve and marker types in the caption part:

In Fig. 2, BLER results are presented under different numbers of codewords U , SNR levels, and numbers of ports N . Several common findings can be summarized: 1) The BLER can be significantly reduced with denser port placement and wider antenna length, i.e., increasing N or W improves the BLER performance, which can easily surpass that of conventional single-antenna systems and even multi-antenna systems. 2) With a sufficiently large number of ports N , the block-correlation channel model provides accurate predictions of BLER performance through the statistical expression in (10), thereby validating both the proposed approach and the accuracy of the block-correlation channel model.

In Fig. 3, the OP performance is illustrated under different SNR values and numbers of active codewords U . The key observations are as follows: 1) The single-antenna MRC

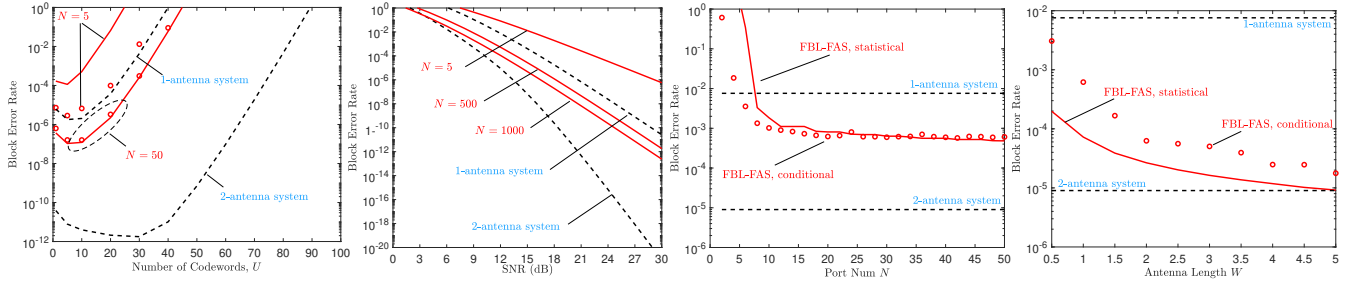


Fig. 2. Illustrations of BLER performance:

-**Different Lines:** Red solid lines denote the statistical BLER of FBL-FAS, red markers represent the corresponding conditional BLER, and black dotted lines indicate the conditional BLER of the conventional L -antenna system.

-**Different Figures:** 1) BLER vs U : $W = 1$, $M = 5$, $N \in \{5, 50\}$, $L \in \{1, 2\}$, and SNR = 20 dB; 2) BLER vs SNR: $W = 0.5$, $M = 5$, $U = 10$, $N \in \{5, 50, 1000\}$, and $L \in \{1, 2\}$; 3) BLER vs N : $W = 1$, $M = 5$, $U = 10$, $L \in \{1, 2\}$, and SNR = 12 dB. 4) BLER vs W : $M = 5$, $U = 10$, $N = 5000$, $L \in \{1, 2\}$, and SNR = 12 dB.

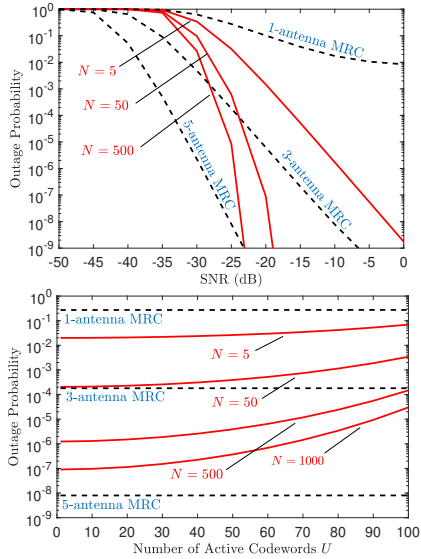


Fig. 3. Illustration of OP performance:

-**Different Lines:** Red solid lines denote the OP of FBL-FAS, while black dotted lines indicate the OP of the MRC system.

-**Different Figures:** Up: OP versus SNR (dB) with $W = 0.5$, $N \in \{5, 50, 500\}$, $L \in \{1, 3, 5\}$, $U = 20$, $M = 5$, and $\gamma_{th} = 10^{-3}$; Down: OP versus the number of codewords U with $W = 0.5$, $N \in \{5, 50, 500, 1000\}$, $L \in \{1, 3, 5\}$ (conventional antenna system), SNR = -35 dB, $M = 5$, and $\gamma_{th} = 10^{-4}$.

system experiences an error floor due to user interference in finite-blocklength transmission. 2) FBL-FAS exhibits a much steeper OP decay as the SNR increases. Notably, even single-antenna FBL-FAS can achieve lower OP than a 5-antenna MRC system when 50 or 500 ports are available. 3) Compared with the 1-antenna MRC system, FBL-FAS achieves 10^7 to 10^4 times lower OP, and it even surpasses the 3-antenna MRC system with approximately 10 times better OP performance.

B. Integral Approximtion

To investigate the impact of μ on the approximation accuracy of different methods, we examine the integral component

$$\int_0^\infty \frac{e^{-\frac{r_b}{2}}}{2} \left[1 - Q_1 \left(\sqrt{\frac{\mu^2 r_b}{1-\mu^2}}, \sqrt{\frac{t}{1-\mu^2}} \right) \right]^{L_b} dr_b$$

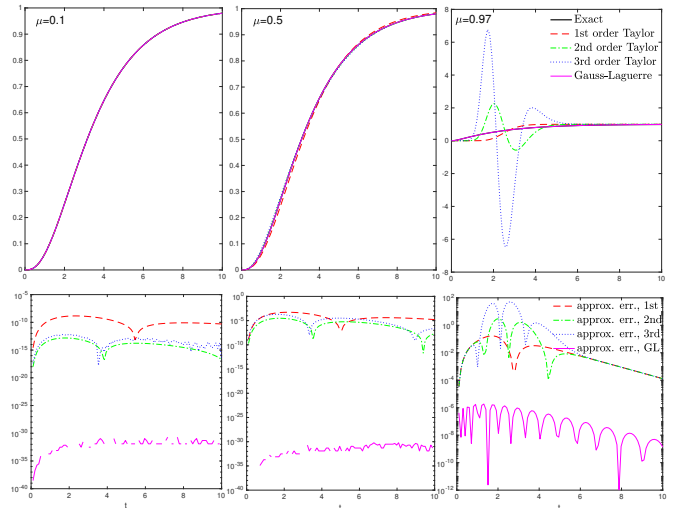


Fig. 4. Illustration of integral approximation under different correlation values in the block-correlation model, using the Taylor expansion-assisted method [3, Theorem 7] and the proposed Gauss-Laguerre method. The figures in the first row show the integral approximation while the figures in the second row show the corresponding approximation error, $|\hat{f}(t) - f(t)|^2$. The x -axis denotes the range of t .

from (13) with $L_b = 3$ and quadrature expansion order of 32, as illustrated in Fig. 4. It can be observed that the Taylor expansion-assisted method becomes inaccurate as μ increases from 0.1 to 0.97. In contrast, the proposed Gauss-Laguerre-based approach remains effective across the entire range of correlation parameters.

V. CONCLUSION

In this work, the performance limits of FBL-FAS [3] are tightly bounded from a statistical perspective by considering the block-correlation channel model in [6]. The PDF expression of the channel gain after port selection is derived and concisely characterized by a non-central chi-square distribution, whose evaluation is further simplified using the Gauss-Laguerre approach to yield accurate approximations. Numerical results validate the tightness of the statistical bounds and highlight the significant spectrum and energy

efficiency achieved by FASs in the FBL regime. Compared with conventional L -antenna systems, FBL-FAS emerges as a promising enabler for future wireless networks.

VI. APPENDIX

A. Proof of Results 1

Remark A-1: Readily converted from [6, Eq. 43], the CDF of random variable $|g_{\text{FAS}}|^2 = \max\{|g_{u,1}|^2, |g_{u,2}|^2, \dots, |g_{u,N}|^2\}$ is:

$$\begin{aligned} F_{|g_{\text{FAS}}|^2} &= P\{|g_{\text{FAS}}|^2 \leq t\} \\ &= \prod_{b=1}^B \int_0^\infty \frac{e^{-\frac{r_b}{2}}}{2} \times \left[1 - Q_1 \left(\sqrt{\frac{\mu^2 r_b}{1-\mu^2}}, \sqrt{\frac{t}{1-\mu^2}} \right) \right]^{L_b} dr_b. \end{aligned} \quad (13)$$

Subsequently, we derive the corresponding PDF by **Remark A-1**. For ease of descriptions, we denote (13) by:

$$F_{|g_{\text{FAS}}|} = \prod_{b=1}^B G_b(t), \quad (14a)$$

$$G_b(t) = \int_0^\infty \frac{1}{2} e^{-r_b/2} [1 - Q_1(a_b(r_b), \sqrt{a_t})]^{L_b} dr_b, \quad (14b)$$

$$a_b(r_b) = \sqrt{\frac{\mu^2}{1-\mu^2} r_b}, \quad \sqrt{a_t} = \sqrt{\frac{t}{1-\mu^2}}. \quad (14c)$$

It is clear that by differentiating CDF, one could obtain the corresponding PDF by $f_{|g_{\text{FAS}}|^2} = \frac{dF_{|g_{\text{FAS}}|^2}}{dt}$. However, to simplify the derivative procedures, the following identities are considered:

- The equivalence between Marcum- Q and non-central chi-square:

$$1 - Q_1(a, \sqrt{x}) = F_{\chi_2^2}(x; a^2), \quad x \geq 0, \quad (15)$$

where $F_{\chi_2^2}(x; a^2)$ is the non-central chi-square CDF with degrees-of-freedom 2 and non-centrality parameter a^2 .

- If x in (15) is a function of variable t , i.e., $x(t)$, the following derivative can be established:

$$\frac{dF_{\chi_2^2}(x(t); a^2)}{dt} = \frac{dx(t)}{dt} f_{\chi_2^2}(x(t); a^2), \quad (16)$$

where $f_{\chi_2^2}(x; a) = \frac{1}{2} e^{-\frac{x+a}{2}} I_0(\sqrt{ax})$ is the corresponding chi-square distribution's PDF.

Thereby, if one consider identity of (15) on (14a) and then use the derivative rule $f_{|g_{\text{FAS}}|^2}(t) \equiv \frac{dF_{|g_{\text{FAS}}|^2}(t)}{dt} = \sum_{b=1}^B \left(\frac{dG_b(t)}{dt} \right) \prod_{j \neq b} G_j(t)$ with identity in (16), (8) is obtained, which completes the proof on **Result 1** in Section III-A.

B. Explanations on Result 2

Different from the constant channel correlation model in [3], the block-approximation model assumes the channel correlation to be a constant close to 1, which aims to capture the correlation among ports in close vicinity. However, when $\mu^2 \rightarrow 1$, if one continues to adopt the "frozen" point integral simplification method in [3, Theorem 7], the approximation

becomes inaccurate due to the limitations of the Taylor expansion in [3, Eq. (56)] for $\mu^2 \rightarrow 1$. Specifically, for the function component $1 - Q_1 \left(\sqrt{\frac{\mu^2 r_b}{1-\mu^2}}, \sqrt{\frac{t}{1-\mu^2}} \right)$ the constant terms $\frac{\mu^2}{1-\mu^2} \rightarrow +\infty$ or $\frac{1}{1-\mu^2} \rightarrow +\infty$ will excessively amplify the higher-order error terms after Taylor expansion, leading to failure of the approximation.

Therefore, it is both useful and interesting to explore ways to compensate for the drawbacks of Taylor-expansion-based methods. In this regard, we introduce how to simplify the integral calculation of expressions with structures similar to (12), inspired by the Gauss-Laguerre quadrature method [7], [8]:

- For an integrand of the form $e^{-x} f(x)$, the integral can be approximated as

$$\int_0^\infty e^{-x} f(x) dx \approx \sum_{i=1}^{N_{GL}} w_i f(x_i), \quad (17)$$

where x_i are the *nodes* and w_i are the corresponding *weights*. The parameter N_{GL} is the expansion order, which determines the approximation accuracy (typically, choosing N_{GL} up to 64 is sufficient).

- According to the Golub-Welsch theorem [7], [8], the values of (x_i, w_i) can be derived by performing an eigenvalue decomposition on the following Jacobi matrix:

$$\mathbf{J} = \begin{pmatrix} \alpha_0 & \sqrt{\beta_1} & 0 & \dots & 0 \\ \sqrt{\beta_1} & \alpha_1 & \sqrt{\beta_2} & \dots & 0 \\ 0 & \sqrt{\beta_2} & \alpha_2 & \dots & 0 \\ \vdots & \vdots & \ddots & \ddots & \sqrt{\beta_{N-1}} \\ 0 & 0 & \dots & \sqrt{\beta_{N-1}} & \alpha_{N-1} \end{pmatrix}, \quad (18)$$

where $\alpha_n = 2n + 1$ and $\beta_n = n^2$.

- The eigenvalue decomposition of (18), i.e., $\mathbf{J} = \mathbf{W}\mathbf{D}\mathbf{W}^T$, provides the nodes x_i as the N largest eigenvalues (diagonal entries of \mathbf{D}). The corresponding weights w_i are obtained from the squared elements of the first row of \mathbf{W} .

REFERENCES

- [1] W. K. New, K.-K. Wong, H. Xu, *et al.*, "A tutorial on fluid antenna system for 6G networks: Encompassing communication theory, optimization methods and hardware designs," *IEEE Commun. Surv. Tutor.*, vol. 27, no. 4, pp. 2325–2377, Nov. 2024.
- [2] K.-K. Wong, A. Shojaefard, K.-F. Tong and Y. Zhang, "Fluid antenna systems," *IEEE Trans. Wireless Commun.*, vol. 20, no. 3, pp. 1950-1962, March 2021.
- [3] Z. Zhang, K.-K. Wong, D. Morales-Jimenez, *et al.*, "Finite-blocklength fluid antenna systems," arXiv, available: [2509.15643](https://arxiv.org/abs/2509.15643)
- [4] Y. Polyanskiy, *et al.*, "Channel coding rate in the finite blocklength regime," *IEEE Trans. Inf. Theory*, vol. 56, no. 5, pp. 2307-2359, May 2010.
- [5] G. Liva and Y. Polyanskiy, "Unsourced multiple access: A coding paradigm for massive random access," *Proc. of the IEEE*, vol. 112, no. 9, pp. 1214-1229, Sept. 2024.
- [6] P. Ramírez-Espinosa, D. Morales-Jimenez and K.-K. Wong, "A new spatial block-correlation model for fluid antenna systems," *IEEE Trans. Wireless Commun.*, vol. 23, no. 11, pp. 15829-15843, Nov. 2024
- [7] William H. Press, Saul A. Teukolsky, *Numerical Recipes 3rd Edition*, Cambridge University Press, Aug., 2007.
- [8] G. H. Golub, J. H. Welsch, "Calculation of gauss quadrature rules," available: <https://web.stanford.edu/class/cme335/spr11/S0025-5718-69-99647-1.pdf>